Flavor Oscillations in the Supernova Hot Bubble Region: Nonlinear Effects of Neutrino Background

Sergio Pastor and Georg Raffelt
Max-Planck-Institut für Physik, Werner-Heisenberg-Institut, Föhringer Ring 6, 80805 Munich, Germany
(Received 16 July 2002; published 22 October 2002)

The neutrino flux close to a supernova core contributes substantially to neutrino refraction so that flavor oscillations become a nonlinear phenomenon. One unexpected consequence is efficient flavor transformation for antineutrinos in a region where only neutrinos encounter a Mikheyev-Smirnov-Wolfenstein resonance or vice versa. Contrary to previous studies we find that in the neutrino-driven wind the electron fraction Y_e always stays below 0.5, corresponding to a neutron-rich environment as required by r-process nucleosynthesis. The relevant range of masses and mixing angles includes the region indicated by LSND, but not the atmospheric or solar oscillation parameters.

DOI: 10.1103/PhysRevLett.89.191101 PACS numbers: 97.60.Bw, 14.60.Pq, 97.10.Cv

Introduction.—The evidence for flavor oscillations of solar and atmospheric neutrinos and in the LSND experiment implies mass differences so small that refractive effects influence or even dominate neutrino oscillations in many situations of practical interest. However, there are only two examples where neutrinos themselves as a medium modify the oscillations. One is the early Universe [1], the other core-collapse supernovae (SNe) [2].

In a seminal paper Pantaleone [3] showed that neutrinos as a background medium differ markedly from other fermions. A given background neutrino may be a coherent superposition of flavor states, implying an "off-diagonal refractive index" in flavor space. The oscillations of the entire ensemble thus become a nonlinear phenomenon with unexpected consequences. When the neutrinos themselves dominate as a background medium, the oscillations become "synchronized"; i.e., all modes oscillate collectively with the same frequency, a behavior first discovered by Samuel [4]. With our collaborators we recently found a simple physical interpretation of this perplexing phenomenon in terms of the dipole-dipole coupling of a collection of magnetic dipoles which spin-precess in an external magnetic field [5].

The first environment where ν-ν refraction plays a crucial role is the epoch of the early Universe that precedes big-bang nucleosynthesis. If initially large flavor-dependent ν-$\bar{\nu}$ asymmetries exist, they may be equilibrated by oscillations and collisions before weak-interaction freeze-out so that the primordial helium abundance implies stringent limits on the overall cosmic neutrino density [6–9]. Depending on initial conditions the modification of the flavor relaxation process caused by the synchronization effect is only mild, or it may even prevent equilibrium entirely because the synchronized oscillation frequency can become arbitrarily small. The interplay of simultaneous ν and $\bar{\nu}$ oscillations is a crucial and nontrivial ingredient in the evolution of this system.

The second system where background neutrinos may be important is the rarefied region just outside the nascent neutron star a few seconds after SN core bounce. In the innermost regions of the SN, the neutrino flux is so large that the weak-interaction potential created by the neutrinos is comparable to that of the ordinary medium. The neutrino spectra and fluxes differ between the flavors and between neutrinos and antineutrinos of a given flavor. Swapping the fluxes of different flavors would crucially modify the production of heavy elements via r-process nucleosynthesis if this phenomenon takes place in the SN hot bubble region [10,11]. The possible importance of ν-ν refraction in this context was quickly recognized [12–14]. The main consequence implied by these approximate treatments was a small shift of the oscillation parameters where a significant spectral swapping by resonant oscillations takes place.

Alerted by the subtleties encountered in our study of early-Universe oscillations [7] we revisit the ν-ν effect in the SN hot bubble region. We find that previous authors indeed underestimated the complications that arise, in particular, when neutrinos and antineutrinos oscillate simultaneously and cause refractive effects for each other. We find, for example, that in a region of parameters where neutrinos encounter a Mikheyev-Smirnov-Wolfenstein (MSW) resonance, the antineutrinos are "dragged along" and also show large flavor transformations. The final picture of the interplay between neutrino oscillations and r-process nucleosynthesis is very different than previously imagined.

Two-flavor system.—To be specific we study the ν_e-ν_μ system with oscillation parameters $\tan^2\theta$ and $\Delta m^2 = m_2^2 - m_1^2 > 0$. In the absence of neutrino background effects, neutrinos (antineutrinos) encounter an MSW resonance for $\tan^2\theta < 1$ ($\tan^2\theta > 1$). The evolution of the neutrino system is described by the 2×2 density matrices

$$\rho_{\mathbf{p}}(t) = \begin{pmatrix} \rho_{ee} & \rho_{e\mu} \\ \rho_{\mu e} & \rho_{\mu\mu} \end{pmatrix} = \frac{1}{2}[P_0(\mathbf{p}, t) + \boldsymbol{\sigma} \cdot \mathbf{P}_{\mathbf{p}}(t)], \quad (1)$$

and analogously $\bar{\rho}_{\mathbf{p}}$ for antineutrinos. Here, σ_i are the

Pauli matrices while $\mathbf{P_p}(t)$ and $\overline{\mathbf{P}}_\mathbf{p}(t)$ are the usual polarization vectors for ν and $\bar{\nu}$ modes with momentum $\mathbf{p}$, respectively. The diagonal elements $\rho_{\alpha\alpha}(\mathbf{p}, t)$ are the occupation numbers of flavor α with momentum $\mathbf{p}$.

In the region of interest neutrinos stream freely so that we may ignore collisions. Therefore, the radial evolution equation is the usual precession formula, augmented by the ν-ν refractive term [15]

$$\partial_r\begin{pmatrix}\mathbf{P_p}\\ \overline{\mathbf{P}}_\mathbf{p}\end{pmatrix} = \left\{\sqrt{2}G_\mathrm{F}\left[N_e\hat{\mathbf{z}} + \int d\mathbf{q}C_\mathbf{pq}(\mathbf{P_q} - \overline{\mathbf{P}}_\mathbf{q})\right] \pm \frac{\Delta m^2}{2p}\mathbf{B}\right\} \times \begin{pmatrix}\mathbf{P_p}\\ \overline{\mathbf{P}}_\mathbf{p}\end{pmatrix}. \quad (2)$$

Here $\mathbf{B} = (\sin 2\theta, 0, -\cos 2\theta)$ is a "magnetic field," θ is the vacuum mixing angle, and $\hat{\mathbf{z}}$ is a unit vector in the z direction in flavor space. Further, $N_e = Y_e N_B$ is the electron density with Y_e the electron fraction and N_B the baryon density. Finally, $C_\mathbf{pq} \equiv 1 - \hat{\mathbf{p}} \cdot \hat{\mathbf{q}}$, implying that collinear neutrinos do not cause a mutual refraction effect.

As a matter density profile for the hot bubble region we use the one shown in Ref. [10] which roughly falls off as r^{-3}. As a boundary condition we assume equal luminosities L_ν for all flavors of order $L_0 \equiv 10^{51}\ \mathrm{erg\,s^{-1}}$. The spectra are taken to be Fermi-Dirac distributions with mean energies $\langle E_{\nu_e}\rangle = 11$ MeV, $\langle E_{\bar{\nu}_e}\rangle = 16$ MeV, and $\langle E_{\nu_\mu,\bar{\nu}_\mu}\rangle = 25$ MeV, respectively. These choices may not be entirely realistic [16], but for consistency with previous work we stick with these traditional assumptions.

In the absence of oscillations and for radially moving neutrinos the diagonal elements of the density matrix at radius r and for neutrino momentum p are

$$\rho_{\alpha\alpha}(p, r) = \frac{L_\nu}{4\pi r^2}\frac{120}{7\pi^4 T_{\nu_\alpha}^4}\frac{p^2}{\exp(p/T_{\nu_\alpha}) + 1}, \quad (3)$$

where $T_{\nu_\alpha} = \langle E_{\nu_\alpha}\rangle/3.151$. For the ν-ν refractive effect the angular divergence of the neutrinos is crucial. As in previous works [13,14] we use a flux-averaged value; i.e., in Eq. (2) we substitute

$$\int d\mathbf{q}\, C_\mathbf{pq}(\mathbf{P_q} - \overline{\mathbf{P}}_\mathbf{q}) \times \mathbf{P_p} \to F(r)\,(\mathbf{P} - \overline{\mathbf{P}}) \times \mathbf{P_p}. \quad (4)$$

Here, $\mathbf{P}$ and $\overline{\mathbf{P}}$ are the total polarization vectors and $F(r) = \frac{1}{2}[1 - (1 - R_\nu^2/r^2)^{1/2}]$ is a geometrical factor with R_ν the neutrino-sphere radius (see [13] for a more detailed discussion of the geometrical dependence). Both $F(r)$ and the luminosity fall off as r^{-2} so that the ν-ν refractive term scales as r^{-4} at large r. In the neutrino-driven wind phase the medium density typically falls off as r^{-3} so that at large distances the ordinary medium dominates. However, at distances of 15–30 km the neutrinos may dominate.

R-process nucleosynthesis.—A key necessary condition for this process to occur in the SN hot bubble region is that the environment must be neutron rich. The neutron-to-proton ratio is fixed by the β processes $\nu_e + n \leftrightarrow p + e^-$ and $\bar{\nu}_e + p \leftrightarrow n + e^+$, while charge neutrality requires $n/p = 1/Y_e - 1$ [10]. Therefore, a minimal requirement is $Y_e < 0.5$, but a successful r process may require $Y_e \lesssim 0.45$. Near weak-interaction freeze-out (WFO), at a radius 30–35 km, only the direct β processes are important and the electron fraction is

$$Y_e \approx \left(1 + \frac{L(\bar{\nu}_e)\bar{\epsilon}}{L(\nu_e)\epsilon}\right)^{-1}, \quad (5)$$

where $\epsilon \equiv \langle E_{\nu_e}^2\rangle/\langle E_{\nu_e}\rangle$ and $\bar{\epsilon}$ is the analog for $\bar{\nu}_e$. We take the ν_e and $\bar{\nu}_e$ cross sections on nucleons to be equal; see, however, [17,18]. In the absence of neutrino oscillations and with our choice of neutrino flux parameters one finds $Y_e \simeq 0.41$, allowing for a successful r process.

Spectral swapping by oscillations.—If neutrino oscillations occur within the WFO radius, the effective ν_e and $\bar{\nu}_e$ flux spectra change and modify Y_e. As a first example we use $\Delta m^2 = 10\ \mathrm{eV}^2$ and $\tan^2\theta = 10^{-3}$ which yield the Y_e profile shown in Fig. 1. For the curve marked 0, neutrino background effects were ignored; the other curves are for the indicated values of L_ν.

The oscillations can be calculated analytically in the limit $L_\nu \gg L_0$ where the neutrino background strongly dominates. We define $\mathbf{I} \equiv \mathbf{P} - \overline{\mathbf{P}}$, integrate Eq. (2) over the neutrino spectra to get the evolution equations for $\mathbf{P}$ and $\overline{\mathbf{P}}$, and subtract them to obtain

$$\partial_r\mathbf{I} = \int d\mathbf{p}\frac{\Delta m^2}{2p}\mathbf{B} \times [\mathbf{P_p} + \overline{\mathbf{P}}_\mathbf{p}] + \sqrt{2}G_\mathrm{F}N_e\hat{\mathbf{z}} \times \mathbf{I}. \quad (6)$$

The neutrino background term is proportional to $\mathbf{I} \times \mathbf{I}$

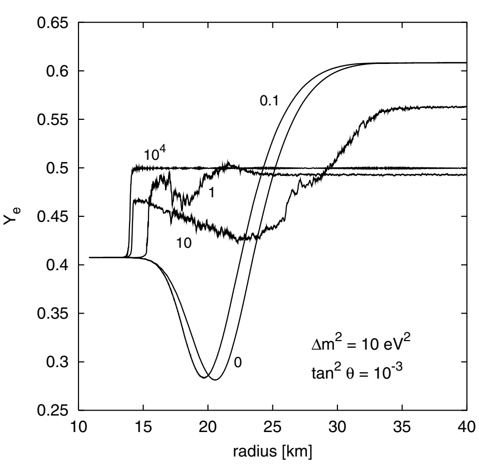

FIG. 1. Y_e as a function of radius for the indicated choice of oscillation parameters. The labels indicate L_ν in units of $L_0 = 10^{51}\ \mathrm{erg\,s^{-1}}$; $L_\nu = 0$ implies the absence of neutrino background effects.

and thus vanishes. However, the individual modes $\mathbf{P_p}$ and $\overline{\mathbf{P}}_\mathbf{p}$ precess fast around $\mathbf{I}$ as in Ref. [5]. The evolution of $\mathbf{I}$ is a slow precession with a certain synchronized frequency $\omega_{\rm synch}$. We express $\omega_{\rm synch}$ by the neutrino momentum $p_{\rm synch}$ that would precess with $\omega_{\rm synch}$ in the absence of a neutrino background. Note that the synchronization of both neutrino and antineutrino modes occurs despite the presence of a CP asymmetric background [8].

To find $p_{\rm synch}$ we use that in the present limit all $\mathbf{P_p}$ and $\overline{\mathbf{P}}_\mathbf{p}$ are essentially aligned with $\mathbf{I}$ so that their projections along $\mathbf{I}$ are conserved. All modes start in the z direction so that altogether $\mathbf{P_p} \simeq P_z(\mathbf{p})\hat{\mathbf{I}}$ and $\overline{\mathbf{P}}_\mathbf{p} \simeq \overline{P}_z(\mathbf{p})\hat{\mathbf{I}}$. We can then rewrite Eq. (6) as

$$\partial_r \mathbf{I} = \left[\frac{\Delta m^2}{2p_{\rm synch}}\mathbf{B} + \sqrt{2}G_{\rm F}N_e\hat{\mathbf{z}}\right]\times\mathbf{I}, \tag{7}$$

where

$$p_{\rm synch} \simeq \frac{18\,\zeta(3)}{\pi^2}\frac{[T_{\nu_e}^{-1} - T_{\bar\nu_e}^{-1}]}{[T_{\nu_e}^{-2} + T_{\bar\nu_e}^{-2} - 2T_{\nu_\mu}^{-2}]}. \tag{8}$$

We have used that initially $T_{\nu_\mu} = T_{\bar\nu_\mu}$. For our assumed spectra we find $p_{\rm synch} \simeq 2.2$ MeV, much smaller than typical energies of the neutrino spectra. As a consequence, neutrino oscillations are effective at smaller radii and for smaller Δm^2 than without a neutrino background, an effect already observed in Refs. [13,14].

The results of Fig. 1 are now easily explained in two limiting cases. Without neutrino background all neutrino modes experience an independent adiabatic MSW transition starting at low energies (Y_e decreases) until the entire ν_e spectrum is swapped with that of ν_μ, leading to the asymptotic value $Y_e \simeq (1 + \langle E^0_{\bar\nu_e}\rangle/\langle E^0_{\nu_\mu}\rangle)^{-1} \simeq 0.61$.

The other limiting case ($L_\nu \gg L_0$) corresponds to a synchronized MSW transition of the entire neutrino and antineutrino ensemble, where all modes follow an adiabatic transition at the same radius where a neutrino with momentum $p_{\rm synch}$ would do an MSW transition in the absence of background neutrinos. Y_e takes on the value 0.5 because both ν_e and $\bar\nu_e$ are swapped with ν_μ and $\bar\nu_\mu$, respectively, and thus take on identical spectra.

For the intermediate cases there is some degree of synchronization, but it is gradually lost at larger radii with the dilution of the neutrino flux. Still for the nominal neutrino luminosity $L_\nu = L_0$ the evolution is quite different from the no-background case.

For our assumed flux spectra we have systematically calculated the effect of spectral swapping as a function of Δm^2 and $\tan^2\theta$. In Fig. 2 we show our results for the assumed luminosities $L_\nu = 0$ (no neutrino background effects), $L_\nu = 0.1$, and $1L_0$. We indicate the region of mixing parameters which is compatible with the experimental results of LSND and KARMEN2 from a joint analysis [19] and the region excluded by Bugey [20].

In the upper panels we show Y_e at the WFO radius $\simeq$ 30 km. In the absence of neutrino background effects ($L_\nu = 0$) our results agree with those from the previous literature [10]. For instance, large Δm^2 and small $\tan^2\theta$ cause $Y_e > 0.5$, violating the minimal requirement for r-process nucleosynthesis. However, such regions gradually disappear when the neutrino background is enhanced; i.e., neutrino background effects prevent Y_e from exceeding 0.5, in stark contrast to the previous literature. Likewise, for an inverted mass situation ($\tan^2\theta > 1$) spectral swapping effects are quite significant even though neutrinos do not encounter an MSW resonance.

Previous studies of the neutrino background effect used various approximations [12–14]. References [13,14] considered the full set of equations in an approximate way but did not include the evolution of antineutrinos. We interpret the fundamental difference between the previous literature and our results as being caused by the simultaneous oscillations of neutrinos and antineutrinos.

Another intriguing aspect of our results is the behavior of $L(\nu_e)$ which we show in the lower panels of Fig. 2 for $r = 50$ km. It is approximately this region where the protons and neutrons of the material which would eventually undergo heavy-element synthesis form alpha particles [21–23]. Therefore, an equal number of protons and neutrons is locked into alphas, the excess of either of them remaining free. But an excess of neutrons can be erased by ν_e capture if $L(\nu_e)$ is large enough ("α effect"). One speculative way of reducing $L(\nu_e)$ invokes oscillations into sterile neutrinos [24–26]. In our case of active-active oscillations there is a range of mixing parameters where $Y_e < 0.5$ at the WFO radius, while at larger radii $L(\nu_e)$ is significantly reduced, thus circumventing the α problem. This happens because the formation of alphas occurs while only the low-energy ν_e's are converted, corresponding to the dips in the Y_e evolution shown in Fig. 1. The relevant region coincides with part of the range allowed by LSND + KARMEN2 and Bugey. However, this effect persists only for relatively small values of L_ν.

Summary.—We find that the impact of neutrino-neutrino refractive effects in the SN hot bubble region differs markedly from the established wisdom. Contrary to a naive expectation, the simultaneous effect of neutrino and antineutrino oscillations is crucial, even if only one of them encounters a resonance. In our calculation the electron fraction Y_e was never enhanced above 0.5 when neutrino background effects were included, thus fulfilling the minimal condition for r-process nucleosynthesis.

If the LSND signature is not due to neutrino conversions and the active-active oscillation parameters permanently settle in the regions indicated by solar and atmospheric neutrino conversions, then it is unlikely that neutrino oscillations influence r-process nucleosynthesis, always assuming the SN hot bubble region is the correct site. There remain interesting oscillation effects at larger radii where the matter density is smaller [27], but

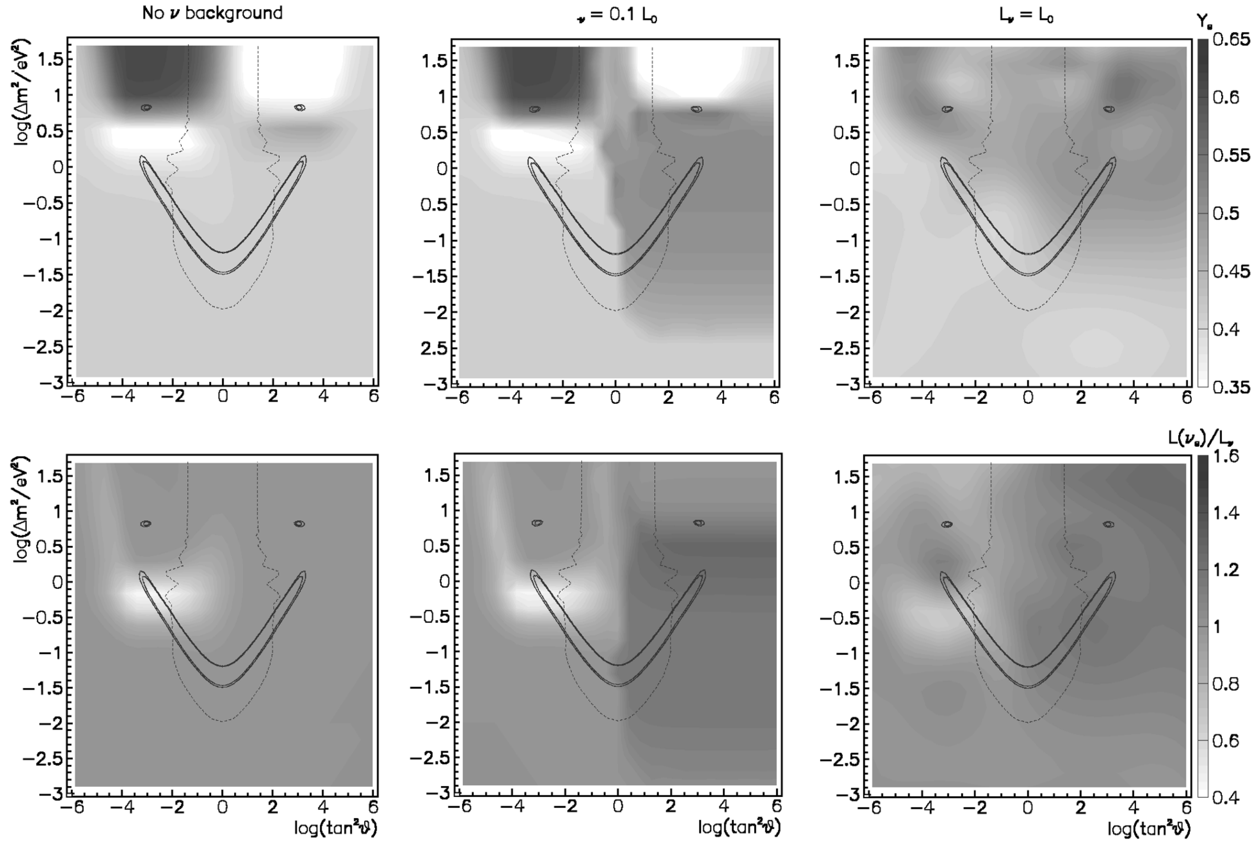

FIG. 2. Spectral swapping as a function of Δm^2 and $\tan^2\theta$ for $L_\nu = 0$ (no neutrino background effects), 0.1, and $1L_0$. The solid contours indicate the LSND + KARMEN2 allowed region [19], while the region inside the dashed contour is excluded by the Bugey experiment [20]. *Upper panels:* Y_e at the WFO radius of $\simeq 30$ km. *Lower panels:* $L(\nu_e)/L_\nu$ at $r = 50$ km.

we do not expect ν-ν refraction to play a major role at these distances. This caveat notwithstanding we find the nonlinear effects of ν-ν refraction in the SN hot bubble region a fascinating topic worth investigating.

We thank A. Dighe, G. Fuller, M. Kachelrieß, M. Maltoni, Y.-Z. Qian, G. Sigl, and R. Tomàs for helpful comments and K. Eitel for sending us the LSND + KARMEN2 data. This work was partly supported by the Deutsche Forschungsgemeinschaft under Grant No. SFB 375 and the ESF Network Neutrino Astrophysics. S. P. was supported by the European Commission under Contract No. HPMFCT-2000-00445.

[1] D. Nötzold and G. Raffelt, Nucl. Phys. **B307**, 924 (1988).
[2] R. Mayle, J. R. Wilson, and D. N. Schramm, Astrophys. J. **318**, 288 (1987).
[3] J. Pantaleone, Phys. Lett. B **287**, 128 (1992).
[4] S. Samuel, Phys. Rev. D **48**, 1462 (1993).
[5] S. Pastor, G. G. Raffelt, and D. V. Semikoz, Phys. Rev. D **65**, 053011 (2002).
[6] C. Lunardini and A. Yu. Smirnov, Phys. Rev. D **64**, 073006 (2001).
[7] A. D. Dolgov *et al.*, Nucl. Phys. **B632**, 363 (2002).
[8] Y. Y. Wong, Phys. Rev. D **66**, 025015 (2002).
[9] K. N. Abazajian, J. F. Beacom, and N. F. Bell, Phys. Rev. D **66**, 013008 (2002).
[10] Y. Z. Qian *et al.*, Phys. Rev. Lett. **71**, 1965 (1993).
[11] Y. Z. Qian, Nucl. Phys. (Proc. Suppl.) **91**, 345 (2000).
[12] J. Pantaleone, Phys. Lett. B **342**, 250 (1995).
[13] Y. Z. Qian and G. M. Fuller, Phys. Rev. D **51**, 1479 (1995).
[14] G. Sigl, Phys. Rev. D **51**, 4035 (1995).
[15] G. Sigl and G. Raffelt, Nucl. Phys. **B406**, 423 (1993).
[16] M. T. Keil, G. Raffelt, and H.-T. Janka, astro-ph/0208035.
[17] C. Horowitz and G. Li, Phys. Rev. Lett. **82**, 5198 (1999).
[18] C. Horowitz, Phys. Rev. D **65**, 083005 (2002).
[19] E. D. Church, K. Eitel, G. B. Mills, and M. Steidl, Phys. Rev. D **66**, 013001 (2002).
[20] B. Achkar *et al.*, Nucl. Phys. **B434**, 503 (1995).
[21] G. M. Fuller and B. S. Meyer, Astrophys. J. **453**, 792 (1995).
[22] G. C. McLaughlin, G. M. Fuller, and J. R. Wilson, Astrophys. J. **472**, 440 (1996).
[23] B. S. Meyer, G. C. McLaughlin, and G. M. Fuller, Phys. Rev. C **58**, 3696 (1998).
[24] G. C. McLaughlin, J. M. Fetter, A. B. Balantekin, and G. M. Fuller, Phys. Rev. C **59**, 2873 (1999).
[25] D. O. Caldwell, G. M. Fuller, and Y. Z. Qian, Phys. Rev. D **61**, 123005 (2000).
[26] J. M. Fetter, G. C. McLaughlin, A. B. Balantekin, and G. M. Fuller, hep-ph/0205029.
[27] R. C. Schirato and G. M. Fuller, astro-ph/0205390.